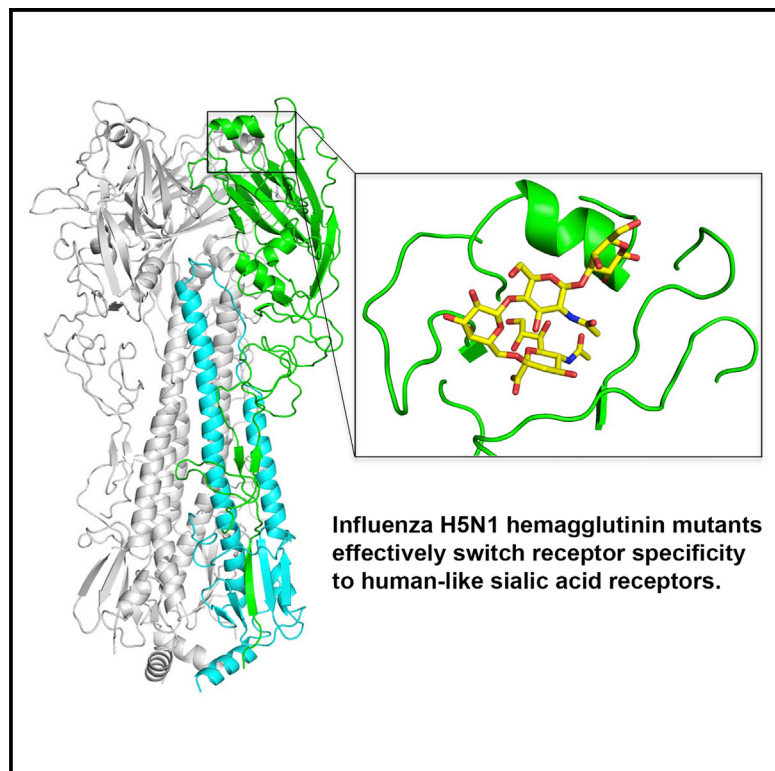


Structural Basis for a Switch in Receptor Binding Specificity of Two H5N1 Hemagglutinin Mutants

Graphical Abstract



Authors

Xueyong Zhu, Karthik Viswanathan, Rahul Raman, Wenli Yu, Ram Sasisekharan, Ian A. Wilson

Correspondence

rams@mit.edu (R.S.), wilson@scripps.edu (I.A.W.)

In Brief

Hemagglutinin receptor binding specificity changes are a prerequisite for influenza viruses to become human transmissible. Zhu et al. report on the structural basis for preferential human receptor binding of two hemagglutinin mutants of H5N1 viruses.

Highlights

- Crystal structures of two H5N1 influenza hemagglutinin mutants
- Receptor specificity of wild-type and mutant H5 hemagglutinins
- Comparison of receptor binding sites of our H5 mutants with ferret-transmissible H5 mutants
- Structural basis for preferential binding of H5 hemagglutinin mutants to human receptors

Accession Numbers

5E2Y
5E2Z
5E30
5E32
5E34
5E35



Structural Basis for a Switch in Receptor Binding Specificity of Two H5N1 Hemagglutinin Mutants

Xueyong Zhu,¹ Karthik Viswanathan,² Rahul Raman,² Wenli Yu,¹ Ram Sasisekharan,^{2,*} and Ian A. Wilson^{1,3,*}

¹Department of Integrative Structural and Computational Biology, The Scripps Research Institute, La Jolla, CA 92037, USA

²Department of Biological Engineering, Koch Institute of Integrative Cancer Research, Infectious Diseases Interdisciplinary Research Group, Singapore-MIT Alliance for Research and Technology, Massachusetts Institute of Technology, Cambridge, MA 02139, USA

³Skaggs Institute for Chemical Biology, The Scripps Research Institute, La Jolla, CA 92037, USA

*Correspondence: rams@mit.edu (R.S.), wilson@scripps.edu (I.A.W.)

<http://dx.doi.org/10.1016/j.celrep.2015.10.027>

This is an open access article under the CC BY-NC-ND license (<http://creativecommons.org/licenses/by-nc-nd/4.0/>).

SUMMARY

Avian H5N1 influenza viruses continue to spread in wild birds and domestic poultry with sporadic infection in humans. Receptor binding specificity changes are a prerequisite for H5N1 viruses and other zoonotic viruses to be transmitted among humans. Previous reported hemagglutinin (HA) mutants from ferret-transmissible H5N1 viruses of A/Vietnam/1203/2004 and A/Indonesia/5/2005 showed slightly increased, but still very weak, binding to human receptors. From mutagenesis and glycan array studies, we previously identified two H5N1 HA mutants that could more effectively switch receptor specificity to human-like α 2-6-linked sialosides with avidity comparable to wild-type H5 HA binding to avian-like α 2-3-linked sialosides. Here, crystal structures of these two H5 HA mutants free and in complex with human and avian glycan receptor analogs reveal the structural basis for their preferential binding to human receptors. These findings suggest continuous surveillance should be maintained to monitor and assess human-to-human transmission potential of H5N1 viruses.

INTRODUCTION

The highly pathogenic H5N1 influenza viruses continue to be a great human health concern. Since 1997, infection with H5N1 viruses has resulted in a very high mortality rate (~60%) among diagnosed and hospitalized patients (http://www.who.int/influenza/human_animal_interface/H5N1_cumulative_table_archives/en/). However, H5N1 infection is generally considered an avian disease, as these viruses have spread extensively among poultry and wild birds, but only occasionally infect humans, usually through direct contact with infected poultry (Ungchusak et al., 2005). Natural H5N1 viruses have not yet acquired the necessary adaptations to establish sustained human-to-human transmission via respiratory droplets (http://www.who.int/influenza/human_animal_interface/avian_influenza/h5n1_research/en/). Notwithstanding, two recent studies of H5

hemagglutinin (HA) mutants of A/Vietnam/1203/2004 (Viet04) (N158D, N224K, Q226L, and T318I, H3 numbering) and A/Indonesia/5/2005 (Ind05) (H110Y, T160A, Q226L, and G228S) showed that it was possible to confer aerosol transmission of H5N1 viruses in ferrets and raised questions of whether the currently circulating H5N1 viruses can acquire such mutations to become transmissible among humans (Herfst et al., 2012; Imai et al., 2012).

The molecular mechanisms of how avian and other zoonotic influenza viruses evolve to cross the species barrier to become airborne-transmissible in humans are not fully understood, but a hallmark of previous influenza pandemics is preferential binding of the virus to human receptors (α 2-6-linked sialoside glycans). The HA on avian viruses must alter its specificity from avian receptors (α 2-3-linked sialosides) to human receptors so as to bind α 2-6-linked sialosides in the upper respiratory tract and also reduce binding to mucins. Thus, it is essential to continuously monitor HA changes in avian viruses that might affect receptor specificity and possible transmission of zoonotic viruses in the human population.

Mutations of H5 HA that affect receptor specificity were identified in previous studies (Chandrasekaran et al., 2008; Chen et al., 2012a; Gambaryan et al., 2006; Stevens et al., 2006, 2008; Watanabe et al., 2011; Yamada et al., 2006). For two ferret-transmissible Viet04 and Ind05 mutant viruses, HA structures and complexes with glycan receptors, as well as glycan array studies, have provided insights into the nature of mutations that skew the preference for human versus avian receptors (de Vries et al., 2014; Lu et al., 2013; Xiong et al., 2013; Zhang et al., 2013). However, none of these mutant H5 HAs showed an effective switch in binding to human receptors that is characteristic of the HAs of pandemic strains (H1, H2, and H3) that infected humans in 1918, 1957, 1968, and 2009 (Tharakaraman et al., 2013). Although these H5 Viet04 and Ind05 mutant viruses or their corresponding HAs preferentially bind human receptors, their binding avidity is much lower compared to the equivalent wild-type virus or other HAs for avian receptors (de Vries et al., 2014; Lu et al., 2013; Xiong et al., 2013; Zhang et al., 2013). The same HA mutations that contribute to aerosol transmission of Viet04 and Ind05 viruses in ferrets would not appear to be sufficient for circulating H5 HAs to efficiently switch their specificity to human receptors (Tharakaraman et al., 2013).

Table 1. Glycan Binding Properties of Wild-Type and Mutant dkEgy10 and ckViet08 H5 HAs^a

	130-Loop Insertion	220 Loop	158 Glycosylation	LSTa	LSTc
dkEgy10 (E5.0)	–	K224, Q226	D158, A160	+++++	–
E5.1	–	K224, <i>L226</i>	D158, A160	–	++++
E5.2	<i>S133a</i>	K224, <i>L226</i>	D158, A160	–	–
E5.3	–	K224, <i>L226</i>	<i>N158, T160</i>	+	–
E5.4	<i>S133a</i>	K224, Q226	D158, A160	+	–
E5.5	<i>S133a</i>	K224, <i>L226</i>	<i>N158, T160</i>	–	–
E5.6	–	K224, Q226	<i>N158, T160</i>	–	–
ckViet08 (V4.4)	–	<i>K224, L226</i>	<i>D158, T160</i>	+	++++
Viet04 mutant	L133a	<i>K224, L226</i>	<i>D158, T160</i>	–	–
Ind05 mutant	<i>S133a</i>	<i>L226, S228</i>	<i>N158, A160</i>	–	–

The mutated residues from wild-type HA are highlighted in italics.

^aThe key RBS residues in H5 HAs for switch of receptor specificity are shown for wild-type dkEgy10 HA (E5.0) and its mutants. Apparent receptor binding on a glycan binding assay: +++++, very strong; +++++, strong; +, weak/variable; –, not detected. Viet04 mutant is the HA of ferret-transmissible A/Vietnam/1203/2004 (with HA mutants N158D, N224K, Q226L, and T318I) (Imai et al., 2012), and Ind05 mutant is the HA of ferret-transmissible A/Indonesia/5/2005 (with mutations H110Y, T160A, Q226L, and G228S) (Herfst et al., 2012).

In a previous study (Tharakaraman et al., 2013), we described a systematic framework to define the H5 HA receptor binding site (RBS) using four structural features. These four features included alteration of the length of the 130 loop (feature 1), alteration of a combination of residue positions in the 130 loop and 220 loop (feature 2), mutations in the 190 helix (feature 3), and removal of a glycosylation sequon at position 158 (feature 4). The feature-based definition of the H5 HA RBS permitted us to identify several H5 HAs from naturally evolving clades that had already acquired one or more of these features and would potentially require fewer amino acid mutations to quantitatively switch their binding to human receptors. Several of these H5 HA mutants that acquired human receptor preference were characterized, including a single Q226L HA mutant (E5.1 HA) from H5N1 virus A/duck/Egypt/10185SS/2010 (dkEgy10, clade 2.2.1) and an HA mutant with N224K, Q226L, N158D, and an L133a deletion (V4.4 HA) from A/chicken/Vietnam/NCVD-093/2008 (ckViet08, clade 7.2). Here, we report the structural basis and further characterization of this effective switch in receptor preference that is afforded by acquisition of human RBS features in H5 E5.1 and V4.4 mutant HAs, and we compare them with corresponding features in other published airborne-transmissible H5 HA mutants as well as HAs from human viruses. Significantly, we show that both E5.1 HA and V4.4 HA bind to human receptor-like glycans in a manner similar to pandemic H2 HA. The structure and network properties of the key RBS residues validate the previously described framework for defining the four molecular features for human receptor binding.

RESULTS

RBS Features Beyond the Single Q226L Mutation Are Critical for the Switch in Receptor Specificity of an HA from a Currently Circulating dkEgy10 H5 Virus

The dkEgy10 HA has avian receptor binding properties, but, after introduction of a single Q226L mutation, the E5.1 HA mutant effectively switches its binding to human receptors, as evidenced by glycan array analysis and physiological glycan receptor binding in human respiratory tissues (Tharakaraman et al., 2013). The dkEgy10 HA had already acquired two of the four RBS features including deletion of residue 133a in the 130 loop (feature 1) and loss of glycosylation at position 158 (feature 4). To understand the contribution of these features beyond the Q226L mutation, we characterized the HA receptor specificity by introducing additional mutations that impacted the four RBS features (Table 1; Figure S1) and then assessed receptor binding using glycan array assays with two natural sialo-pentasaccharides from human milk, LSTa (NeuAc α 2-3Gal β 1-3GlcNAc β 1-3Gal β 1-4Glc) and LSTc (NeuAc α 2-6Gal β 1-4GlcNAc β 1-3Gal β 1-4Glc), which are analogs of avian and human receptors, respectively (Eisen et al., 1997). Consistent with previous results using other linear glycans (Tharakaraman et al., 2013), introduction of a Q226L mutation (E5.1, feature 2) quantitatively switched dkEgy10 HA binding from LSTa to LSTc with only slightly lower comparative avidity. However, insertion of S133a to E5.1 HA in the 130 loop (E5.2, impacting feature 1) completely abrogated binding to both LSTa and LSTc. Similarly, the addition of glycosylation at position 158 (E5.3, impacting feature 4) completely eliminated binding of E5.1 HA to LSTc, but weak binding was retained to LSTa. Therefore, despite the presence of the prototypic Q226 (associated with avian receptor binding) or L226 (associated with human receptor binding), additional amino acid changes that impact one or more of features 1, 2, and 4 (E5.4, E5.5 and E5.6) resulted in almost full elimination of E5.1 HA binding to LSTc and weak or no affinity to LSTa.

By comparison, the mutant of ckViet08 HA (V4.4 HA) exhibits potent binding to LSTc but limited binding to LSTa (Table 1). In contrast, the ferret-transmissible Viet04 and Ind05 mutant HAs display very weak or no obvious binding to either LSTc or LSTa in our receptor binding analyses (Table 1).

Crystal Structures of E5.1 and V4.4 HAs in a Complex with a Human Receptor Analog

To provide structural insights for the receptor specificity switch afforded by RBS features in different H5 HA clades, we determined crystal structures of E5.1 and V4.4 HAs in their apo form and in complex with human receptor analog LSTc (Table 2). In the E5.1 HA complex with LSTc, four of the five glycan moieties (Sia-1, Gal-2, GlcNAc-3, and Gal-4) are well ordered as indicated by clear, interpretable electron density (Figures 1A, S2A, and 2A). Sia-1 is stabilized by hydrogen bonds to Tyr98, Val135, Ser136, Ser137, and Glu190. Furthermore, the 3-carboxyl group of Gal-2 is located within hydrogen bonding distance of Lys222. LSTc adopts a *cis/gauche* conformation (Xu et al., 2009) about the glycosidic bond with sialic acid, with a Sia-1-Gal-2 linkage Φ angle (torsion angle between C1, C2 atoms of Sia-1 and O6, C6 atoms of Gal-2 for LSTc) of -46.4° (the ideal *cis/gauche* Φ

Table 2. Data Collection and Refinement Statistics for E5.1 and V4.4 H5 HA

Dataset	E5.1/apo	E5.1/LSTa	E5.1/LSTc	V4.4/apo	V4.4/LSTa	V4.4/LSTc
Space group	P2 ₁	P2 ₁	P2 ₁	P6	P6	P6
Unit cell (Å)	a = 70.8, b = 235.8, c = 71.5	a = 73.1, b = 234.2, c = 72.9	a = 69.9, b = 228.5, c = 70.7	a = b = 133.0, c = 134.7	a = b = 130.8, c = 133.4	a = b = 130.3, c = 133.6
β angle (deg.)	β = 114.4	β = 115.5	β = 114.3			
Resolution (Å) ^a	50.0-2.60 (2.64-2.60)	50.0-2.60 (2.64-2.60)	50.0-2.70 (2.76-2.70)	50.0-2.70 (2.75-2.70)	50.0-2.70 (2.76-2.70)	50.0-2.70 (2.76-2.70)
X-ray source	SSRL 12-2	APS 23ID-B	APS 23ID-B	APS 23ID-B	APS 23ID-B	APS 23ID-B
Unique reflections	57,168	57,187	52,960	33,778	34,678	34,751
Redundancy ^a	2.4 (1.7)	3.3 (3.0)	2.6 (2.4)	6.2 (6.3)	7.5 (5.2)	7.4 (4.8)
Average I/σ(I) ^a	15.3 (1.5)	17.1 (1.6)	15.7 (1.6)	29.9 (1.9)	13.5 (1.2)	18.5 (1.3)
Completeness ^a	86.8 (67.1)	89.4 (87.6)	94.9 (91.5)	90.5 (90.4)	98.1 (79.4)	97.9 (77.5)
R _{sym} ^{a,b}	0.09 (0.46)	0.11 (0.88)	0.07 (0.67)	0.15 (0.41)	0.16 (0.71)	0.13 (0.63)
R _{pim} ^{a,b}	0.07 (0.43)	0.07 (0.51)	0.05 (0.53)	0.13 (0.32)	0.06 (0.29)	0.05 (0.27)
CC _{1/2} ^a	0.992(0.628)	0.993(0.563)	0.996(0.588)	0.998(0.688)	0.997(0.864)	0.998(0.871)
HA protomers in a.u.	3	3	3	1	1	1
V _m (Å ³ /Da)	3.2	3.3	3.0	6.0	5.7	5.7
Reflections in refinement	57,100	57,132	52,908	33,771	34,531	34,581
Refined residues	1,494	1,494	1,494	498	498	498
Refined waters	179	167	160	139	90	49
Refined ligand atoms	—	108	171	—	46	46
R _{cryst} ^c	0.196	0.202	0.201	0.197	0.214	0.230
R _{free} ^d	0.236	0.249	0.249	0.232	0.250	0.270
B-values (Å ²)						
Protein	59	59	46	65	54	68
Ligand	—	66	51	—	68	76
Waters	39	41	23	53	46	59
Wilson B-values (Å ²)	52	55	57	71	48	55
Ramachandran values (%) ^e	94.2, 0	94.7, 0.1	95.3, 0.1	93.1, 0.6	93.5, 1.0	92.8, 0.4
rmsd bond (Å)	0.010	0.010	0.010	0.008	0.008	0.008
rmsd angle (°)	1.29	1.30	1.27	1.18	1.17	1.13
PDB code	5E2Y	5E2Z	5E30	5E32	5E34	5E35

a.u., asymmetric unit.

^aParentheses denote outer-shell statistics.

^b $R_{\text{sym}} = \sum_{hkl} \sum_i |I_{hkl,i} - \langle I_{hkl} \rangle| / \sum_{hkl} \sum_i I_{hkl,i}$ and $R_{\text{pim}} = \sum_{hkl} [1/(N-1)]^{1/2} \sum_i |I_{hkl,i} - \langle I_{hkl} \rangle| / \sum_{hkl} \sum_i I_{hkl,i}$, where $I_{hkl,i}$ is the scaled intensity of the i^{th} measurement of reflection h, k, l , $\langle I_{hkl} \rangle$ is the average intensity for that reflection, and N is the redundancy. $R_{\text{pim}} = \sum_{hkl} (1/(n-1))^{1/2} \sum_i |I_{hkl,i} - \langle I_{hkl} \rangle| / \sum_{hkl} \sum_i I_{hkl,i}$, where n is the redundancy.

^c $R_{\text{cryst}} = \sum_{hkl} |F_o - F_c| / \sum_{hkl} |F_o|$, where F_o and F_c are the observed and calculated structure factors.

^d R_{free} was calculated as for R_{cryst} but on 5% of data excluded before refinement.

^eThe values are percentage of residues in the favored and outliers regions analyzed by MolProbity (Chen et al., 2010).

angle is -60°). For long α 2-3-linked and α 2-6-linked glycans, the θ angle between the C2 atom of Sia-1 and the C1 atoms of Gal-2 and GlcNAc-3 has been proposed to be a parameter describing glycan topology, with a cone-like topology ($\theta > 110^\circ$) for long α 2-3-linked glycans and an umbrella-like topology ($\theta < 110^\circ$) for long α 2-6-linked glycans (Chandrasekaran et al., 2008; Xu et al., 2009). In the E5.1 HA/LSTc complex, the θ angle of the LSTc is $\sim 84.0^\circ$, indicating an umbrella-like topology. No significant backbone conformational changes arise in E5.1 HA on binding to LSTc, and only a few potentially noteworthy side-chain rotamer changes are observed, such as for Arg193 (Figure 2B).

In the V4.4 HA/LSTc complex (Table 2), Sia-1, Gal-2, and GlcNAc-3 are well ordered (Figures 1C, S2C, and 2C). The Sia-1 moiety hydrogen bonds with HA1 Val135, Ser136, Ser137, and Glu190. LSTc is in *cis/gauche* conformation with a Sia-1-Gal-2 Φ angle of -45.1° , similar to that in the E5.1/LSTc complex. The glycan topology θ angle of LSTc is 82.6° , again indicating an umbrella-like topology. Upon binding to LSTc, no large conformational changes are observed in the V4.4 HA RBS except for a slight movement of the Met193 side chain (Figure 2D). The E5.1 HA and V4.4 HA structures superimpose well, with a C_α root-mean-square deviation (rmsd) of 0.6 Å for

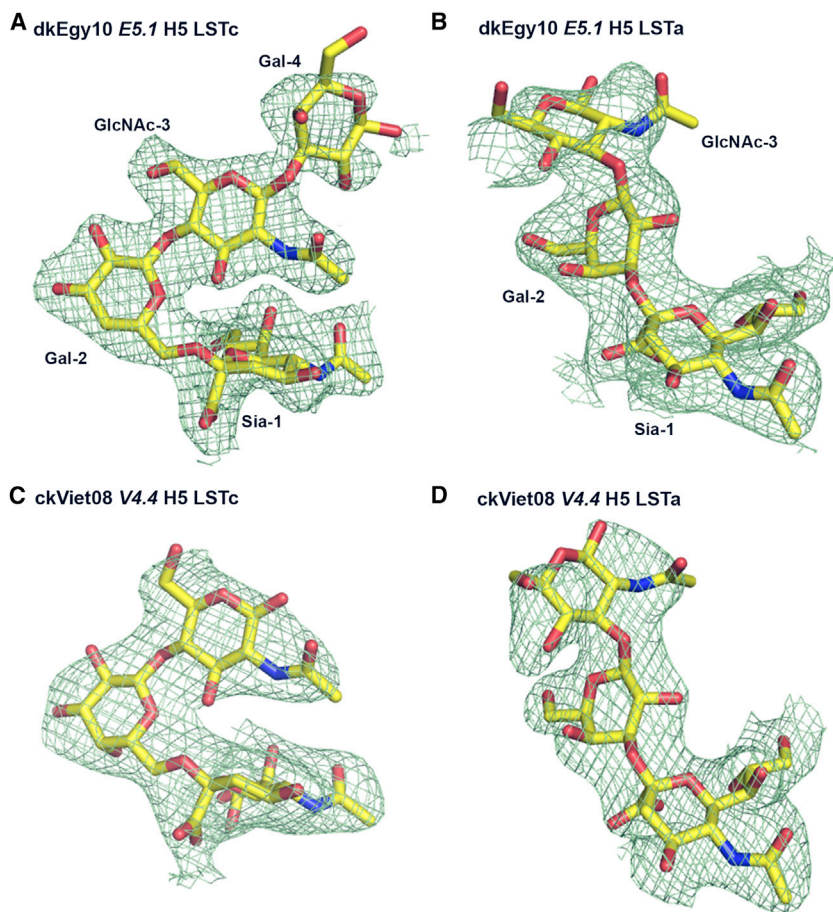


Figure 1. Final 2Fo-Fc Electron Density Maps of Glycan Ligands Bound in H5 HA Crystal Structures

(A) LSTc in *E5.1* HA (2.7 Å resolution).
 (B) LSTa in *E5.1* HA (2.6 Å resolution).
 (C) LSTc in *V4.4* HA (2.7 Å resolution).
 (D) LSTa in *V4.4* HA (2.7 Å resolution).
 The electron density for the glycan receptors is represented in a green mesh and contoured at 0.9 σ . (For omit maps, please see Figure S2.)

the receptor binding subdomain (residues 117–265) (Ha et al., 2002), and the LSTc conformations also closely resemble one another (Figure 3A).

The receptor binding subdomain of HA in *E5.1* HA/LSTc complex was then compared with LSTc complexes of Viet04 mutant HA (PDB code 4KDO) (Lu et al., 2013) and Ind05 mutant HA (PDB: 4K67) (Zhang et al., 2013), as well as H2 HA (PDB: 2WR7) (Liu et al., 2009) (Figure 3). Significantly, when *E5.1* HA (or *V4.4* HA) structures are superimposed with H2 HA (C_α rmsds of 1.0 Å and 0.9 Å for the receptor binding subdomain, respectively), the LSTc ligands closely overlap (Figure 3B). However, when *E5.1* HA was superimposed with Viet04 mutant HA/LSTc (Figure 3C) or Ind05 mutant HA/LSTc (Figure 3D) (C_α rmsd values of 0.9 Å and 0.5 Å for the receptor binding subdomain, respectively), the LSTc GlcNAc-3 moiety was found to have shifted significantly.

The glycan topology θ angles of LSTc in *E5.1* HA (84.0°) and *V4.4* HA (82.6°) are similar in the H2 HA (82.9°) but more disparate with LSTc in the Viet04 mutant HA (98.0°) and Ind05 mutant HA (92.5°). The LSTc conformations in Viet04 and Ind05 mutant HAs are similar, with the GlcNAc-3 exiting the RBS further from the 190 helix compared to three other HA structures discussed above.

It is noteworthy that the Viet04 and Ind05 mutant HAs have Ser133a and Leu133a insertions in the 130 loop, respectively (Figures 3B, 3C, and S1). The main-chain carbonyl oxygen of res-

idue 133a is ~ 3.1 Å from the *N*-acetyl group of Sia-1 in both LSTc complexes with Viet04 and Ind05 mutant HAs, indicating close van der Waals interactions. On the other hand, in *E5.1* HA and *V4.4* HA, as well as in H2 HA, no 133a insertions are present, and all atoms in the 130 loop are more than 3.6 Å away from the Sia-1 *N*-acetyl group. The role of the 133a insertion in receptor binding has been investigated in previous studies (Tharakaraman et al., 2013), as well as here (Table 1), and indicates that insertion of Ser133a in *E5.1* HA or Leu133a in *V4.4* HA almost completely abrogates receptor binding to both avian and human receptors.

Crystal Structures of *E5.1* HA and *V4.4* HA in Complexes with Avian Receptors

Although *E5.1* HA and *V4.4* HA bind weakly to the avian-type receptor LSTa in glycan

array studies, crystal soaking with very high concentrations (10 mM) of LSTa in the crystallization buffer enabled LSTa complexes of *E5.1* HA and *V4.4* HA to be determined (Table 2). In the crystal structure of *E5.1* HA with avian receptor analog LSTa (Table 2), electron density for only three of the five glycan moieties (Sia-1, Gal-2, and GlcNAc-3) of LSTa are observed (Figures 4A, 1B, and S2B). Sia-1 is stabilized by hydrogen bonds with Tyr98, Val135, Ser136, Ser137, Glu190, and Arg193. LSTa binds in a *cis/gauche* conformation (Xu et al., 2009), as indicated by the Sia-1-Gal-2 linkage Φ angle (torsion angle between C1, C2 atoms of Sia-1 and O3, C3 atoms of Gal-2 for LSTa) of -60.7° , close to a perfect *cis/gauche* conformation. Interestingly, when *E5.1* HA binds LSTa, the C_α atoms of 220-loop residues 223–226 move away from the RBS by ~ 1.0 Å (Figure 4B), which has not been reported for any other H5 HAs.

Similarly, the structure of *V4.4* HA in complex with LSTa (Table 2) revealed that LSTa also adopts a *cis/gauche* conformation with the Sia-1-Gal-2 linkage Φ angle of -47.9° (Figures 4C, 1D, and S2D) and no major conformational changes arise in *V4.4* HA upon LSTa binding (Figure 4D).

The LSTa conformations in *E5.1* and *V4.4* HA complexes are superimposable and similar to that in the Ind05 mutant HA LSTa complex (PDB: 4K66) (Zhang et al., 2013), which was also in *cis/gauche* conformation with a Φ angle of -63.0° (Figure 5). The Viet04 mutant in complex with LSTa was not used

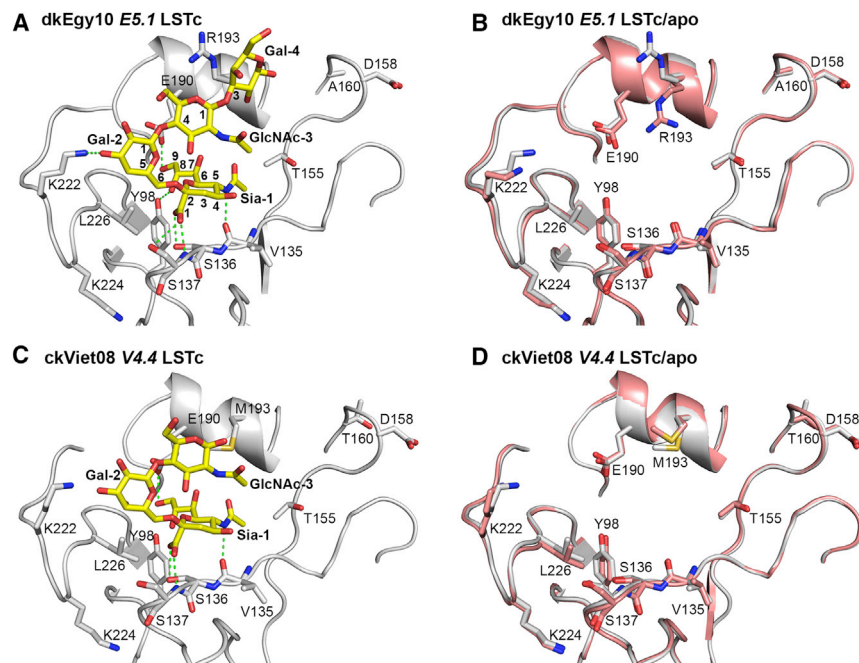


Figure 2. Crystal Structures of E5.1 and V4.4 H5 HAs and Their Complexes with Human Receptor Analog LSTc

(A) The receptor binding site (RBS) of E5.1 HA (gray tubes for the backbone with selected residues in the binding site shown in atomic representation with gray carbon atoms, blue nitrogen atoms, and red oxygen atoms) in complex with human receptor analog LSTc (yellow carbon atoms, blue nitrogen atoms, and red oxygen atoms).

(B) Structural comparison of the RBS of E5.1 HA (gray carbon atoms) in complex with LSTc versus apo-E5.1 HA (pink carbon atoms) with glycan ligand removed for clarity.

(C) The RBS of V4.4 HA bound with human receptor analog LSTc. The coloring scheme is similar to that of (A).

(D) Structural comparison of the RBSs of V4.4 HA in complex with LSTc versus apo-V4.4 HA with glycan ligand removed. The coloring scheme is the same as (B).

for comparison as LSTa is not well ordered with electron density observed only for Sia-1 (Lu et al., 2013). The GlnAc-3 of LSTa in E5.1 and V4.4 HA complexes exits from the side of RBS over the 220 loop. In contrast, LSTa in the wild-type H5 HA VN1194 complex (PDB: 3ZP0) (Crusat et al., 2013) adopts a *trans/anti* conformation with a Φ angle of $\sim 170.8^\circ$ (the preferred *trans/anti* Φ angle is 180°) with its Gal-2 projecting out of the RBS (Figure 5D).

Interestingly, Asn169 and Asn167 in E5.1 HA and V4.4 HA are observed to be glycosylated (Figures 5A and 5B). These sugars might result in a steric clash with natural $\alpha 2$ -3-linked avian glycans receptors bound to the neighboring HA protomer within an HA trimer, which would be biologically relevant.

DISCUSSION

Influenza virus transmission is an important component of the proposed gain-of-function mutants of avian influenza viruses and provides valuable information for virus surveillance and pandemic preparedness (Fouchier et al., 2013). As the first step in influenza infection, binding of the HA to human cell-surface receptors with appropriate affinity and specificity is a crucial requirement for viral infection and spread as well as for assessing human pandemic potential. In previous studies, two H5N1 influenza viruses with mutant HAs were airborne transmissible among ferrets (Herfst et al., 2012; Imai et al., 2012), raising concerns for possible human-to-human transmission. However, further studies revealed that, although these mutant HAs greatly decreased affinity to avian receptors, they only slightly increased affinity for human receptors (de Vries et al., 2014; Lu et al., 2013; Xiong et al., 2013; Zhang et al., 2013) (Table 1). Here, we report on crystal structures of E5.1 and V4.4 H5 HAs, which can effectively switch substrate specificity from avian to human receptors with comparable binding affinity.

E5.1 and V4.4 HAs both have Lys224 and Leu226 in their RBS as well as loss of N-linked glycosylation at 158 on the RBS rim, all of which are signatures of ferret-transmissible Viet04 HA (Imai et al., 2012). While Lys224 is believed to enhance virus binding to the carboxylate group of the receptor sialic acid through electrostatic interaction (Xiong et al., 2013), Leu226 is the key signature residue for human receptor binding in both ferret-transmissible Viet04 and Ind05 HAs as well as in human H2 and H3 HAs (Herfst et al., 2012; Imai et al., 2012). In E5.1 HA, a Q226L mutation from wild-type dkEgy10 HA effectively switches its receptor specificity. In avian H5 HA, the hydrophilic Gln226 interacts with the glycosidic oxygen of LSTa but creates an unfavorable environment for the nonpolar portion of the $\alpha 2$ -6 linkage of LSTc (Xiong et al., 2013; Zhang et al., 2013). On the contrary, in the transmissible H5 HA mutant and in the two other H5 HAs here with Leu226, the hydrophobic Leu226 creates an unfavorable environment for interaction with the hydrophilic portion of LSTa but increases hydrophobic interactions with the nonpolar part of the LSTc $\alpha 2$ -6 linkage. Removal of the 158 glycosylation appears to decrease steric hindrance to access to the binding site for human receptors (Stevens et al., 2008; Wang et al., 2010).

Significantly, both E5.1 HA and V4.4 HA bind LSTc in a manner similar to pandemic H2 HA (Figure 3), the nearest human-adapted phylogenetic neighbor in group-1 HAs, providing further evidence that the natural evolution of H5 HA RBS might follow an H2-like path (Tharakaraman et al., 2013). Similar to H2 HA, there is no insertion of a 133a residue in E5.1 HA and V4.4 HA, thereby representing a major difference in the RBS with that of Viet04 and Ind05 mutant HAs, which have Leu133a and Ser133a, respectively (Figure S1). Insertion of a residue at 133a into E5.1 HA (Table 1) and V4.4 HAs (Tharakaraman et al., 2013) almost completely abrogates binding to both avian and human receptors. The 133a deletion together with I155T has been reported to increase binding to human receptors for another H5 HA A/duck/Egypt/D1Br12/2007 (H5N1) (Watanabe et al., 2011),

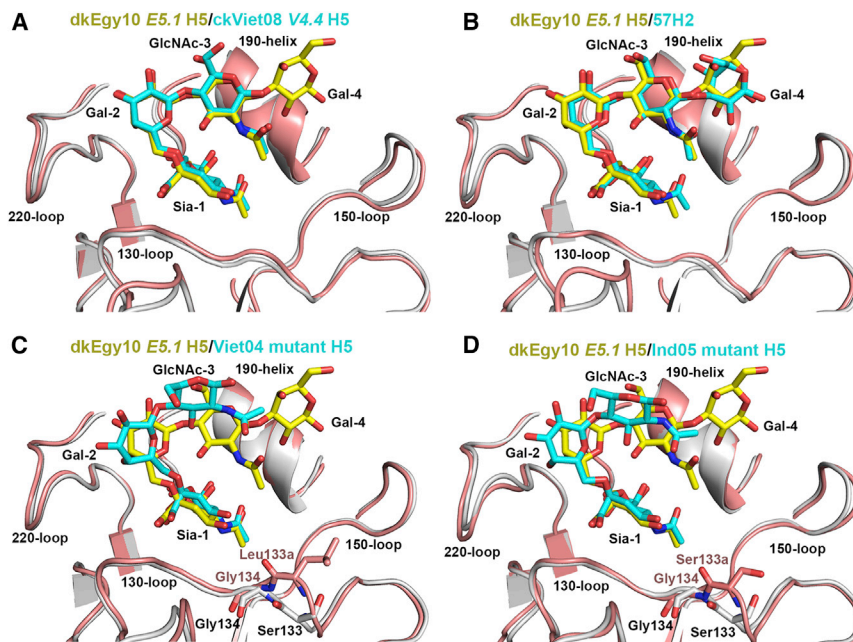


Figure 3. Structural Comparison of LSTc bound to E5.1 H5 HA with Other HAs

The receptor binding subdomain (residues 117–265) was used to superimpose HA structures. (A) Superimposition of the RBS of E5.1 HA (gray) with LSTc (yellow carbon atoms) and the RBS of V4.4 H5 HA (pink) with LSTc (cyan carbon atoms). The same coloring scheme is used in (B)–(D). (B) Superimposition of the RBS of E5.1 HA with LSTc and human H2 HA with LSTc (PDB: 2WR7). (C) Superimposition of the RBS of E5.1 HA with LSTc and Viet04 mutant H5 HA with LSTc (PDB: 4KDO). The side chain of Leu133a insert of Viet04 mutant HA is shown in pink carbon atoms. (D) Superimposition of the RBS of E5.1 HA with LSTc and Ind05 mutant H5 HA with LSTc (PDB: 4K67). The side chain of Ser133a insert of Ind05 mutant HA is shown in pink carbon atoms. All panels are shown in the same orientation.

whereas removal of the 133a insertion increases avidity for both avian and human receptors in an H1 HA (Koerner et al., 2012). These results together highlight the importance of analyzing the impact of amino-acid mutations (or substitutions) in the context of the features around the RBS that critically affect glycan receptor binding properties of H5 HA.

Upon binding to E5.1 HA or V4.4 HA, LSTa adopts a *cis/gauche* conformation and exits the RBS over the 220-loop in an extended conformation in contrast to wild-type VN1194 (A/Vietnam/1194/2004) H5 HA where LSTa adopts a *trans/anti* conformation. In E5.1 HA or V4.4 HA, LSTa is bound such that long mammalian glycans at positions 169 (E5.1 HA) or 167 (V4.4 HA) of an adjacent HA protomer within the HA trimer would sterically block binding of LSTa or other avian glycans attached to the host cell surface, consistent with a computational analysis that suggested large glycans at position 169 would be more effective in preventing binding of α 2-3-Sia-Gal analogs (Chen et al., 2012b). Thus, although the relatively short LSTa structures, which were obtained by soaking HA crystals at very high ligand concentrations (mM), exhibit binding to LSTa, the HA on the virus might not be able to productively bind avian glycans on the host cell surface at physiological levels. Furthermore, identification of glycosylation sites on adjacent HA protomers that impact receptor binding warrants expansion on the RBS feature definition to take into account the entire trimeric HA.

In proposed feature 3, residues in the 190-helix, such as at position 193, could be involved in binding to LSTc. E5.1 HA has an Arg193, while V4.4 has Met193. However, both HAs bind strongly to human receptors, indicating tolerance for the 193 side chain, in contrast to a previous hypothesis that the long Arg193 might push LSTc away from the receptor binding site (Zhang et al., 2013).

The crystal structures of V4.4 and E5.1 H5 HAs provide valuable templates for building models of H5 HAs that lack the

key RBS residues (see Tharakaraman et al., 2013 for details) in the mutant H5 HAs. Interestingly, mapping of the topological connectivity of key RBS residues, based on amino-acid interaction network scores of the different HAs, indicates E5.1 HA is more similar to H2 HA than Viet04 H5 HA (Figure S3). The closeness of network properties of key RBS residues of E5.1 HA and H2 HA validates the framework for defining the four molecular features based on comparison with H2 HA RBS.

The determination of mutant H5 HA structures with Leu at position 226 motivated a search in the H5 HA sequence space to identify sequences that have evolved to naturally acquire the Q226L mutation. This search identified a single strain isolated from Cambodia in 2013 (A/Cambodia/X0810301/2013, Cam13) that has naturally acquired this mutation in addition to an N224K mutation. These two amino-acid changes are key to acquire feature 2 of H2 HA RBS. Cam13 HA has substantially reduced binding to avian receptor (LSTa), but did not switch specificity to human receptor (LSTc) in a dose-dependent direct binding assay (data not shown). This observation is consistent with other observations in Table 1 where acquiring feature 2 alone is not sufficient to achieve the receptor specificity switch. Cam13 H5 HA belongs to clade 1.1 and is more similar to clade 1 sequences like Viet04 than to clade 2.2.1 or clade 7 sequences (Figure S4). Therefore, despite the natural acquisition of the Q226L mutation, the Cam13 HA would require more amino-acid substitutions than dkEg10 to switch its specificity.

In summary, we have structurally characterized two H5 HA mutants that completely switch substrate specificity from avian to human receptors. Influenza virus infection among individuals or between species is a complex process, but HA binding to the human receptors is the first major committed step. For E5.1 HA, which represents a current circulating H5 strain, only one Q226L mutation was needed to effectively switch specificity from avian to human receptors. Further experiments in animals

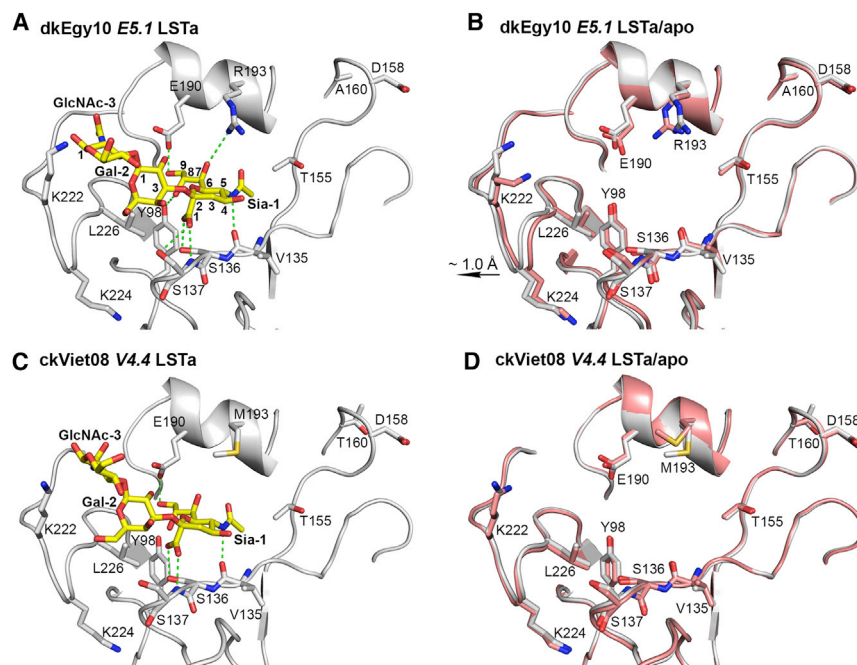


Figure 4. Crystal Structures of E5.1 and V4.4 H5 HA and in Complex with Avian Receptor Analog LSTa

(A) The RBS of E5.1 HA with avian receptor analog LSTa.

(B) Structural comparison of the RBSs of E5.1 HA in complex with LSTa versus apo-E5.1 HA with glycan ligand removed.

(C) The RBS of V4.4 HA bound with avian receptor analog LSTa.

(D) Structural comparison of the RBSs of V4.4 HA in complex with LSTa versus apo-V4.4 HA with glycan ligand removed.

The coloring scheme is the same as Figure 2.

and virus surveillance data are needed to confirm the pandemic potential of viruses that acquire such mutations in the H5 HA. The H5 HA structures defined here along with the previously defined feature-based classification of H5 RBS provide a valuable tool for surveillance of H5N1 viruses and for assessing its evolution toward human adaptation.

EXPERIMENTAL PROCEDURES

Cloning, Baculovirus Expression, and Purification of HA for Crystallization

The ectodomains of E5.1 and V4.4 HAs were expressed in a baculovirus system essentially as previously described (Tharakaraman et al., 2013; Zhu et al., 2013a, 2013b). Briefly, the cDNAs corresponding to residues 11–327 of HA1 and 1–174 of HA2 (H3 numbering) of wild-type dkEgy10 HA (GenBank: JN807780) and ckViet08 H5 HA (GenBank: FJ842480) were codon-optimized and synthesized for insect cell expression and inserted into a baculovirus transfer vector (pAcGP67A, BD Biosciences), with an N-terminal gp67 signal peptide and a C-terminal trimerization domain followed by a His₆ tag, with a thrombin cleavage site between the HA ectodomain and the trimerization domain/His tag. Once sequence verified, the plasmid was used for mutation studies. The recombinant baculoviruses were created using Baculogold system (BD Biosciences) according to manufacturer's instructions in Sf9 cells. HA protein was produced in suspension cultures of Hi5 cells with recombinant baculovirus at an MOI of 5–10 and incubated at 28°C shaking at 110 rpm. After 72 hr, Hi5 cells were removed by centrifugation and supernatants containing secreted, soluble HA proteins were concentrated and buffer-exchanged into 1 × PBS (pH 7.4). The HAs consisted of a mixture of uncleaved HA0 and cleaved HA1/HA2, and were recovered from the cell supernatants by metal affinity chromatography using Ni-NTA resin. The HA was treated with trypsin to produce uniformly cleaved HA1/HA2 and to remove the trimerization domain and His₆ tag. The cleaved HA was further purified by size exclusion chromatography on a Hiloal 16/90 Superdex 200 column (GE Healthcare) in 10 mM Tris (pH 8.0), 50 mM NaCl, and 0.02% (v/v) Na₂S₂O₅.

Crystallization, Data Collection, and Structural Determination

Crystallization experiments were set up using the sitting drop vapor diffusion method. Initial crystallization conditions for E5.1 and V4.4 HAs were obtained

from robotic crystallization trials using our automated Rigaku CrystalMation system at the Joint Center for Structural Genomics (JCSG). Following optimization, diffraction-quality crystals of E5.1 HA were obtained by mixing 0.5 μl of concentrated protein (5.0 mg/ml) in 10 mM Tris (pH 8.0), 50 mM NaCl with 0.5 μl of a reservoir solution containing 0.085 M Tris (pH 8.5), 10% (v/v) glycerol, 0.17% (w/v) sodium acetate, and 21% (w/v) PEG4000 at 22°C. The crystals were flash-cooled in liquid nitrogen without additional cryoprotectant. E5.1 HA-ligand complexes

were obtained by soaking HA crystals in the well solution that now contained glycan ligands. Final concentrations of ligands LSTa (NeuAc₂-3Galβ1-3GlcNAcβ1-3Galβ1-4Glc), and LSTc (NeuAc₂-6Galβ1-4GlcNAcβ1-3Galβ1-4Glc) were all 10 mM, and soaking times were 1 hr and 10 min for LSTa and LSTc, respectively. Diffraction data were collected on synchrotron radiation sources specified in the data statistics tables. HKL-2000 (HKL Research) was used to integrate and scale diffraction data. Initial phases were determined by molecular replacement using Phaser (McCoy et al., 2005) with the Viet04 HA structure (PDB: 3GBM) as a model. One HA trimer is present per asymmetric unit. Refinement was carried out using the program Phenix (Adams et al., 2010). Model rebuilding was performed manually using the graphics program Coot (Emsley et al., 2010). Final refinement statistics are summarized in Table 2.

Diffraction-quality crystals of V4.4 HA were grown at 22°C by mixing 0.5 μl protein (11.5 mg/ml) in 10 mM Tris (pH 8.0), 50 mM NaCl with 0.5 μl of a reservoir solution containing 0.2 M ammonium acetate and 20% (w/v) PEG3350. The crystals were flash-cooled in liquid nitrogen by adding 30% (v/v) ethylene glycol to the mother liquor as cryoprotectant. V4.4 HA-ligand complexes were obtained by soaking LSTa and LSTc at 10 mM final concentration in cryo-solution for 10 min. Data collection and structural determination were similar to those described above for E5.1 HA. Only one HA protomer of the trimer was present in the crystal asymmetric unit. Final refinement statistics are summarized in Table 2.

Cloning, Mammalian Expression, and Purification of HA for Ligand Binding Studies

Mutant HAs were made by site-directed mutagenesis with the H5 wild-type template. The primers for mutagenesis were designed using QuikChange Primer Design and synthesized by IDT DNA technologies. The mutagenesis reaction was carried out using the QuikChange II Site-Directed Mutagenesis Kit as per the manufacturer's instructions. The HAs described here had the polybasic site between HA1 and HA2 replaced by a single Arg and, as such, were expressed as HA0 with no cleavage. Recombinant expression of HA was carried out in HEK293-F FreeStyle suspension cells (Invitrogen) cultured in 293-F FreeStyle Expression Medium (Invitrogen) maintained at 37°C, 80% humidity and 8% CO₂. Cells were transfected with polyethyleneimine "Max" (PEI "Max", PolySciences) with the HA plasmid and were harvested seven days post-infection. The supernatant was collected by centrifugation, filtered through a 0.45-μm filter system (Nalgene), and supplemented with 1:1,000

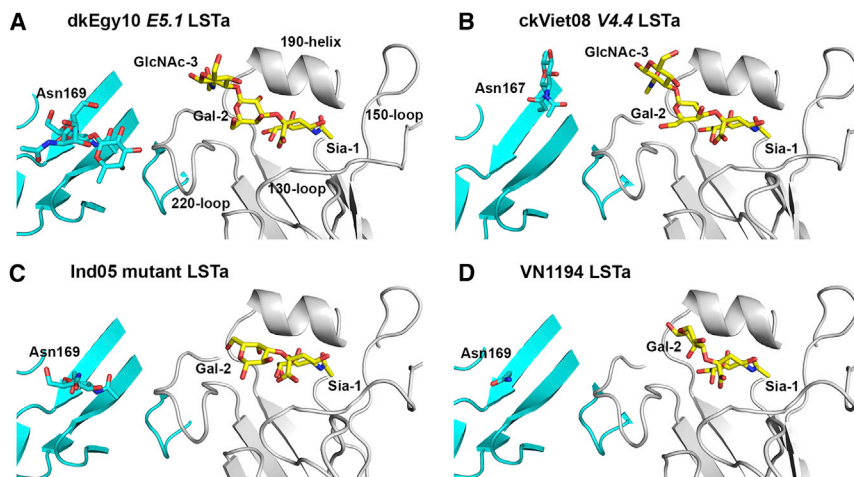


Figure 5. Structural Comparison of LSTa Bound to H5 HAs

(A) The RBS of *E5.1* HA (gray backbone) with LSTa (yellow carbon atoms) and a neighboring protomer within the same HA trimer is shown in cyan. The *N*-glycosylation site Asn169 and its *N*-linked glycans from the neighboring HA protomer are highlighted in sticks. The same coloring scheme is used in (B)–(D).

(B) The RBS of *E4.4* HA with LSTa. The *N*-glycosylation site now at Asn167 and *N*-linked glycans from the neighboring HA protomer are highlighted.

(C) The RBS of Ind05 mutant HA with LSTa (PDB code 4K66). The RBS of *E4.4* HA with LSTa. The *N*-glycosylation site at Asn169 and *N*-linked glycans from the neighboring HA protomer are highlighted.

(D) The RBS of VN1194 native HA with LSTa (PDB code 3ZP0). The *N*-glycosylation site at Asn169 from the neighboring HA protomer is highlighted. All panels were generated in the same orientation.

diluted protease inhibitor cocktail (EMD Millipore). HA was purified from the supernatant using His-trap columns (GE Healthcare) on an AKTA Purifier FPLC system. Eluting fractions containing HA were pooled, concentrated and buffer exchanged into 1× PBS (pH 7.4) using 100K MWCO spin columns (Millipore). The purified protein was quantified using BCA method (Pierce).

Dose-Dependent Direct Binding of HA to LSTa and LSTc

To investigate the multivalent HA-glycan interactions, a streptavidin-coated 384-well plate was coated with biotinylated α 2-3 or α 2-6 sialylated glycans as described previously (Hobbie et al., 2013). Briefly, LSTc and LSTa were biotinylated with EZ-Link Biotin-LC-Hydrazide (Thermo Scientific) according to the manufacturer's instructions, and the biotinylated glycans were collected on a GlykoClean G Cartridge (Prozyme) and further purified with a GLYCOSEP N HPLC column (Prozyme). The purified glycan fraction was lyophilized, reconstituted twice in water to remove residual salts, analyzed by MALDI-TOF, and quantified by both a Sialic Acid Quantification Kit (Prozyme) and a HABA Biotin Quantitation Kit (AnaSpec). The dose-dependent glycan binding assay was carried out as described previously (Srinivasan et al., 2008). Streptavidin-coated High Binding Capacity 384-well plates (Pierce, Rockford, IL) were loaded by incubating each well with 50 μ l of 2.4 μ M of biotinylated glycans overnight at 4°C. Excess glycans were removed through extensive washing with PBS at room temperature (~22°C).

HA naturally exists in a trimeric form, but the spatial arrangement of biotinylated glycan on the streptavidin plates promotes binding of only one of the monomers of the trimeric HA with the glycan. To enhance multivalent HA-glycan interaction, the HA was complexed with primary and secondary antibodies in a molar ratio of 4:2:1 (HA: primary: secondary). This pre-complexation facilitated arrangement of four trimeric HA units in the complex. A stock solution containing His-tagged HA protein, primary antibody (mouse anti 6X His-tag immunoglobulin G [IgG], Abcam) and secondary antibody (horse-radish-peroxidase [HRP]-conjugated goat anti-mouse IgG, Santa Cruz Biotechnology) in the ratio 4:2:1 was incubated on ice for 20 min. The pre-complexed stock HA at 40 μ g/ml was diluted serially diluted with 1% BSA in PBS. 50 μ l of this diluted pre-complexed HA was added to LSTc- and LSTa-coated wells and incubated at room temperature for 2 hr followed by the three washes with PBST (1× PBS + 0.1% Tween-20) and three washes with PBS. The binding signal was determined based on HRP activity using Amplex Red Peroxidase Assay (Invitrogen) according to the manufacturer's instructions.

ACCESSION NUMBERS

The accession numbers for the atomic coordinates and structure factors reported in this paper are PDB: 5E2Y, 5E2Z, and 5E30 for *E5.1* H5 in *apo* form and in complex with LSTa and with LSTc and PDB: 5E32, 5E34, and 5E35 for *V4.4* H5 in *apo* form and in complex with LSTa and with LSTc. Validation

reports for all of the structures can be accessed from the Protein Data Bank (PDB) by using the accession codes.

SUPPLEMENTAL INFORMATION

Supplemental Information includes four figures and can be found with this article online at <http://dx.doi.org/10.1016/j.celrep.2015.10.027>.

ACKNOWLEDGMENTS

We thank Henry Tien of the Robotics Core at the Joint Center for Structural Genomics for automated robotic crystal screening. This work was supported by NIH grant U54 GM094586, NIH grant R56 AI099275 (I.A.W.), the Skaggs Institute for Chemical Biology, NIH Merit Award R37 GM057073-13 (R.S.), NIAID R01AI111395 (R.S.), National Research Foundation supported Interdisciplinary Research group in Infectious Diseases of SMART (Singapore MIT alliance for Research and Technology) (R.S.), and the Skolkovo Foundation supported Infectious Diseases Center at MIT (R.S.). X-ray diffraction data were collected at the Advanced Photon Source (APS) beamline 23ID-B (GM/CA CAT) and the Stanford Synchrotron Radiation Lightsource (SSRL) beamline 12-2. GM/CA CAT is funded in whole or in part with federal funds from the National Cancer Institute (Y1-CO-1020) and the National Institute of General Medical Sciences (Y1-GM-1104). Use of the APS was supported by the U.S. Department of Energy, Basic Energy Sciences, Office of Science, under contract no. DE-AC02-06CH11357. The SSRL is a Directorate of SLAC National Accelerator Laboratory and an Office of Science User Facility operated for the U.S. Department of Energy Office of Science by Stanford University. The SSRL Structural Molecular Biology Program is supported by the DOE Office of Biological and Environmental Research and by the NIH, the National Institute of General Medical Sciences (NIGMS; including P41GM103393), and the National Center for Research Resources (NCRR; P41RR001209). The contents of this publication are solely the responsibility of the authors and do not necessarily represent the official views of the National Institute of Allergy and Infectious Diseases, NIGMS, NCRR, or NIH. This is publication 28045 from The Scripps Research Institute.

Received: August 25, 2015

Revised: October 5, 2015

Accepted: October 8, 2015

Published: November 12, 2015

REFERENCES

Adams, P.D., Afonine, P.V., Bunkóczi, G., Chen, V.B., Davis, I.W., Echols, N., Headd, J.J., Hung, L.W., Kapral, G.J., Grosse-Kunstleve, R.W., et al. (2010).

- PHENIX: a comprehensive Python-based system for macromolecular structure solution. *Acta Crystallogr. D Biol. Crystallogr.* **66**, 213–221.
- Chandrasekaran, A., Srinivasan, A., Raman, R., Viswanathan, K., Raguram, S., Tumpey, T.M., Sasisekharan, V., and Sasisekharan, R. (2008). Glycan topology determines human adaptation of avian H5N1 virus hemagglutinin. *Nat. Biotechnol.* **26**, 107–113.
- Chen, V.B., Arendall, W.B., 3rd, Headd, J.J., Keedy, D.A., Immormino, R.M., Kapral, G.J., Murray, L.W., Richardson, J.S., and Richardson, D.C. (2010). MolProbity: all-atom structure validation for macromolecular crystallography. *Acta Crystallogr. D Biol. Crystallogr.* **66**, 12–21.
- Chen, L.M., Blixt, O., Stevens, J., Lipatov, A.S., Davis, C.T., Collins, B.E., Cox, N.J., Paulson, J.C., and Donis, R.O. (2012a). In vitro evolution of H5N1 avian influenza virus toward human-type receptor specificity. *Virology* **422**, 105–113.
- Chen, W., Sun, S., and Li, Z. (2012b). Two glycosylation sites in H5N1 influenza virus hemagglutinin that affect binding preference by computer-based analysis. *PLoS ONE* **7**, e38794.
- Crusat, M., Liu, J., Palma, A.S., Childs, R.A., Liu, Y., Wharton, S.A., Lin, Y.P., Coombs, P.J., Martin, S.R., Matrosovich, M., et al. (2013). Changes in the hemagglutinin of H5N1 viruses during human infection—influence on receptor binding. *Virology* **447**, 326–337.
- de Vries, R.P., Zhu, X., McBride, R., Rigter, A., Hanson, A., Zhong, G., Hatta, M., Xu, R., Yu, W., Kawaoka, Y., et al. (2014). Hemagglutinin receptor specificity and structural analyses of respiratory droplet-transmissible H5N1 viruses. *J. Virol.* **88**, 768–773.
- Eisen, M.B., Sabesan, S., Skehel, J.J., and Wiley, D.C. (1997). Binding of the influenza A virus to cell-surface receptors: structures of five hemagglutinin-sialyloligosaccharide complexes determined by X-ray crystallography. *Virology* **232**, 19–31.
- Emsley, P., Lohkamp, B., Scott, W.G., and Cowtan, K. (2010). Features and development of Coot. *Acta Crystallogr. D Biol. Crystallogr.* **66**, 486–501.
- Fouchier, R.A., Kawaoka, Y., Cardona, C., Compans, R.W., Garcia-Sastre, A., Govorkova, E.A., Guan, Y., Herfst, S., Orenstein, W.A., Peiris, J.S., et al. (2013). Gain-of-function experiments on H7N9. *Science* **341**, 612–613.
- Gambaryan, A., Tuzikov, A., Pazynina, G., Bovin, N., Balish, A., and Klimov, A. (2006). Evolution of the receptor binding phenotype of influenza A (H5) viruses. *Virology* **344**, 432–438.
- Ha, Y., Stevens, D.J., Skehel, J.J., and Wiley, D.C. (2002). H5 avian and H9 swine influenza virus haemagglutinin structures: possible origin of influenza subtypes. *EMBO J.* **21**, 865–875.
- Herfst, S., Schrauwen, E.J., Linster, M., Chutinimitkul, S., de Wit, E., Munster, V.J., Sorrell, E.M., Bestebroer, T.M., Burke, D.F., Smith, D.J., et al. (2012). Airborne transmission of influenza A/H5N1 virus between ferrets. *Science* **336**, 1534–1541.
- Hobbie, S.N., Viswanathan, K., Bachelet, I., Aich, U., Shriver, Z., Subramanian, V., Raman, R., and Sasisekharan, R. (2013). Modular glycosphere assays for high-throughput functional characterization of influenza viruses. *BMC Biotechnol.* **13**, 34.
- Imai, M., Watanabe, T., Hatta, M., Das, S.C., Ozawa, M., Shinya, K., Zhong, G., Hanson, A., Katsura, H., Watanabe, S., et al. (2012). Experimental adaptation of an influenza H5 HA confers respiratory droplet transmission to a reassortant H5 HA/H1N1 virus in ferrets. *Nature* **486**, 420–428.
- Koerner, I., Matrosovich, M.N., Haller, O., Staeheli, P., and Kochs, G. (2012). Altered receptor specificity and fusion activity of the haemagglutinin contribute to high virulence of a mouse-adapted influenza A virus. *J. Gen. Virol.* **93**, 970–979.
- Liu, J., Stevens, D.J., Haire, L.F., Walker, P.A., Coombs, P.J., Russell, R.J., Gamblin, S.J., and Skehel, J.J. (2009). Structures of receptor complexes formed by hemagglutinins from the Asian Influenza pandemic of 1957. *Proc. Natl. Acad. Sci. USA* **106**, 17175–17180.
- Lu, X., Shi, Y., Zhang, W., Zhang, Y., Qi, J., and Gao, G.F. (2013). Structure and receptor-binding properties of an airborne transmissible avian influenza A virus hemagglutinin H5 (VN1203mut). *Protein Cell* **4**, 502–511.
- McCoy, A.J., Grosse-Kunstleve, R.W., Storoni, L.C., and Read, R.J. (2005). Likelihood-enhanced fast translation functions. *Acta Crystallogr. D Biol. Crystallogr.* **61**, 458–464.
- Srinivasan, A., Viswanathan, K., Raman, R., Chandrasekaran, A., Raguram, S., Tumpey, T.M., Sasisekharan, V., and Sasisekharan, R. (2008). Quantitative biochemical rationale for differences in transmissibility of 1918 pandemic influenza A viruses. *Proc. Natl. Acad. Sci. USA* **105**, 2800–2805.
- Stevens, J., Blixt, O., Tumpey, T.M., Taubenberger, J.K., Paulson, J.C., and Wilson, I.A. (2006). Structure and receptor specificity of the hemagglutinin from an H5N1 influenza virus. *Science* **312**, 404–410.
- Stevens, J., Blixt, O., Chen, L.M., Donis, R.O., Paulson, J.C., and Wilson, I.A. (2008). Recent avian H5N1 viruses exhibit increased propensity for acquiring human receptor specificity. *J. Mol. Biol.* **381**, 1382–1394.
- Tharakaraman, K., Raman, R., Viswanathan, K., Stebbins, N.W., Jayaraman, A., Krishnan, A., Sasisekharan, V., and Sasisekharan, R. (2013). Structural determinants for naturally evolving H5N1 hemagglutinin to switch its receptor specificity. *Cell* **153**, 1475–1485.
- Ungchusak, K., Auewarakul, P., Dowell, S.F., Kitphati, R., Auwanit, W., Puthavathana, P., Uiprasertkul, M., Boonnak, K., Pittayawonganon, C., Cox, N.J., et al. (2005). Probable person-to-person transmission of avian influenza A (H5N1). *N. Engl. J. Med.* **352**, 333–340.
- Wang, W., Lu, B., Zhou, H., Suguitan, A.L., Jr., Cheng, X., Subbarao, K., Kemble, G., and Jin, H. (2010). Glycosylation at 158N of the hemagglutinin protein and receptor binding specificity synergistically affect the antigenicity and immunogenicity of a live attenuated H5N1 A/Vietnam/1203/2004 vaccine virus in ferrets. *J. Virol.* **84**, 6570–6577.
- Watanabe, Y., Ibrahim, M.S., Ellakany, H.F., Kawashita, N., Mizuike, R., Hiramatsu, H., Sriwilajaroen, N., Takagi, T., Suzuki, Y., and Ikuta, K. (2011). Acquisition of human-type receptor binding specificity by new H5N1 influenza virus sublineages during their emergence in birds in Egypt. *PLoS Pathog.* **7**, e1002068.
- Xiong, X., Coombs, P.J., Martin, S.R., Liu, J., Xiao, H., McCauley, J.W., Locher, K., Walker, P.A., Collins, P.J., Kawaoka, Y., et al. (2013). Receptor binding by a ferret-transmissible H5 avian influenza virus. *Nature* **497**, 392–396.
- Xu, D., Newhouse, E.I., Amaro, R.E., Pao, H.C., Cheng, L.S., Markwick, P.R., McCammon, J.A., Li, W.W., and Arzberger, P.W. (2009). Distinct glycan topology for avian and human sialopentasaccharide receptor analogues upon binding different hemagglutinins: a molecular dynamics perspective. *J. Mol. Biol.* **387**, 465–491.
- Yamada, S., Suzuki, Y., Suzuki, T., Le, M.Q., Nidom, C.A., Sakai-Tagawa, Y., Muramoto, Y., Ito, M., Kiso, M., Horimoto, T., et al. (2006). Haemagglutinin mutations responsible for the binding of H5N1 influenza A viruses to human-type receptors. *Nature* **444**, 378–382.
- Zhang, W., Shi, Y., Lu, X., Shu, Y., Qi, J., and Gao, G.F. (2013). An airborne transmissible avian influenza H5 hemagglutinin seen at the atomic level. *Science* **340**, 1463–1467.
- Zhu, X., Guo, Y.H., Jiang, T., Wang, Y.D., Chan, K.H., Li, X.F., Yu, W., McBride, R., Paulson, J.C., Yuen, K.Y., et al. (2013a). A unique and conserved neutralization epitope in H5N1 influenza viruses identified by an antibody against the A/Goose/Guangdong/1/96 hemagglutinin. *J. Virol.* **87**, 12619–12635.
- Zhu, X., Yu, W., McBride, R., Li, Y., Chen, L.M., Donis, R.O., Tong, S., Paulson, J.C., and Wilson, I.A. (2013b). Hemagglutinin homologue from H17N10 bat influenza virus exhibits divergent receptor-binding and pH-dependent fusion activities. *Proc. Natl. Acad. Sci. USA* **110**, 1458–1463.